Ultrafast structural changes in $SrTiO_3$ due to a superconducting phase transition in a $YBa_2Cu_3O_7$ top layer

To cite this article: A Lübcke *et al* 2010 *New J. Phys.* **12** 083043

New Journal of Physics
The open-access journal for physics

Ultrafast structural changes in $SrTiO_3$ due to a superconducting phase transition in a $YBa_2Cu_3O_7$ top layer

A Lübcke[1,3,7], F Zamponi[1,3], R Loetzsch[1], T Kämpfer[1], I Uschmann[1], V Große[2], F Schmidl[2], T Köttig[2,4], M Thürk[2], H Schwoerer[1,5], E Förster[1], P Seidel[2] and R Sauerbrey[1,6]

[1] Institut für Optik und Quantenelektronik, Friedrich-Schiller-Universität Jena, Max-Wien-Platz 1, 07743 Jena, Germany

[2] Institut für Festkörperphysik, Friedrich-Schiller-Universität Jena, Max-Wien-Platz 1, 07743 Jena, Germany

E-mail: luebcke@mbi-berlin.de

New Journal of Physics **12** (2010) 083043 (11pp)
Received 16 March 2010
Published 24 August 2010
Online at http://www.njp.org/
doi:10.1088/1367-2630/12/8/083043

Abstract. We investigate the structural response of $SrTiO_3$ when Cooper pairs are broken in an epitaxially grown $YBa_2Cu_3O_7$ top layer due to both heating and optical excitation. The crystal structure is investigated by static, temperature-dependent and time-resolved x-ray diffraction. In the static case, a large strain field in $SrTiO_3$ is formed in the proximity of the onset of the superconducting phase in the top layer, suggesting a relationship between both effects. For the time-dependent studies, we likewise find a large fraction of the probed volume of the $SrTiO_3$ substrate strained if the top layer is superconducting. Upon optical breaking of Cooper pairs, the observed width of the rocking curve is reduced and its position is slightly shifted towards smaller angles. The dynamical theory of x-ray diffraction is used to model the measured rocking curves. We find that the thickness of the strained layer is reduced by about 200 nm on a sub-ps to ps timescale, but the strain value at the interface between $SrTiO_3$ and $YBa_2Cu_3O_7$ remains unaffected.

[3] Current address: Max-Born-Institut, Max-Born-Straße 2A, 12489 Berlin, Germany.

[4] Current address: Cern Cryolab, CH-1211, Geneve 23, Switzerland.

[5] Current address: Laser Research Institute, University of Stellenbosch, Private Bag X1, 7602 Matieland, South Africa.

[6] Current address: Forschungszentrum Dresden-Rossendorf, Bautzner Landstraße 400, 01328 Dresden, Germany.

[7] Author to whom any correspondence should be addressed.

Contents

1. Introduction

Plasmas created by intense femtosecond (fs) laser pulses are known to be a source of ultrashort bursts of characteristic x-radiation. In the past, they have been used to study acoustic and optical phonons [1]–[4], structural phase transitions [5]–[8], zone-folded acoustic phonons in nanostuctures [9], polarization dynamics in ferroelectric nanolayers [10], dipole solvation dynamics in molecular crystals [11] and magnetostriction in ferromagnets [12] by time-resolved x-ray diffraction. Recently, a plasma-based x-ray source was employed to obtain time-resolved powder diffraction patterns [13]. With time-resolved x-ray diffraction, in principle, the atomic positions in a crystalline material can be tracked in time with a pm spatial and approximately 100 fs temporal resolution.

In this work, we apply this technique to investigate the effect of ultrafast Cooper-pair breaking in a superconducting $YBa_2Cu_3O_7$ top layer on the crystal structure of the $SrTiO_3$ substrate. $SrTiO_3$ is an incipient ferroelectric; nevertheless, ferroelectricity can be induced by electric fields [14], by uniaxial strain [15] and by epitaxial strain [16, 17] due to a thin top-layer like $YBa_2Cu_3O_7$. The $YBa_2Cu_3O_7/SrTiO_3$ contact electronically forms a Schottky contact, which gives rise to an electric field in the $SrTiO_3$. Due to the piezoelectric effect, this leads to a strain gradient in the bulk material close to the $YBa_2Cu_3O_7/SrTiO_3$ interface. Breaking of Cooper pairs is an ultrafast process [18]–[20] with a typical time constant of a few 100 fs. Previous work with Cooper-pair breaking spectroscopy has shown that Cooper pairs in $YBa_2Cu_3O_7$ are efficiently broken with 1.5 eV photons [21].

This experiment provides evidence for strain formation in $SrTiO_3$ due to the superconductivity of the $YBa_2Cu_3O_7$ layer. We show by time-resolved x-ray diffraction that the thickness of the strained layer in the substrate decreases on a timescale of about 1 ps upon Cooper-pair breaking by a pump laser.

2. The experimental setup

For these experiments, a 250 nm thin $YBa_2Cu_3O_7$ film was epitaxially grown on a single-crystalline $SrTiO_3$ substrate. The crystalline quality of the sample was previously examined by means of standard x-ray diffraction techniques. An $\omega/2\theta$ scan revealed a single c-oriented phase for both the thin film and the substrate. In order to monitor the superconducting state of the probed volume, the sample was structured with a meander-like pattern to allow for a resistive

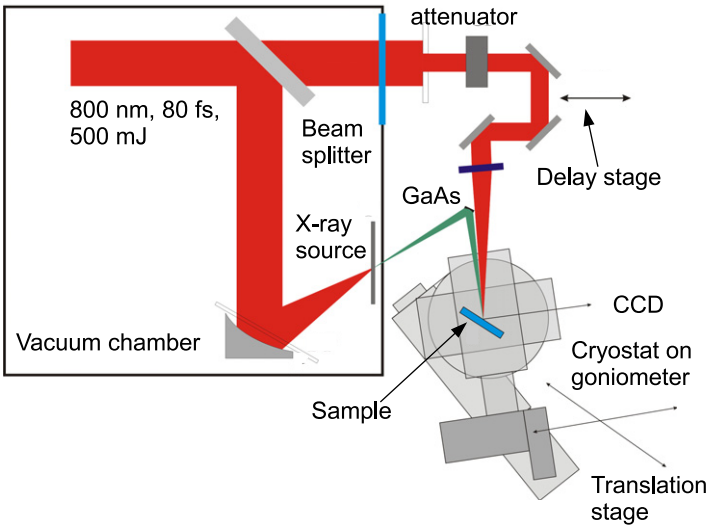

Figure 1. The experimental setup.

measurement, which was run after each data point. The meander had a width of 100 μm. The superconducting transition temperature after the experiment was unchanged and measured as 89 K. The sample was cooled by a commercially available Stirling-type cryostat down to about 70 K. The temperature stability was better than 1 K.

Information about the time-dependent crystal structure was inferred from the reflection of an ultrashort x-ray pulse emitted from a plasma source. The photon energy was 4.5 keV (Ti-Kα_1); the pulse duration can be estimated to be of the order of 300 fs [8]. The extinction depth for the x-ray pulse is about 500 nm in each material, i.e. only an interface-near region will be probed.

Experiments were performed with a 10 Hz Ti:sapphire laser system supplying pulses of 800 nm, 80 fs and 500 mJ. The principal experimental setup is shown in figure 1. The main fraction of the laser pulse (90%) is focused by an off-axis parabolic mirror onto a Ti-tape target, where it generates a hot plasma, which emits characteristic Kα radiation. A fraction of the nearly isotropically emitted radiation is collected, monochromatized and refocused onto the sample by a toroidally bent GaAs (100) crystal. The incidence divergence on the sample is about 2°; therefore, the full reflection curve can be obtained without rocking the sample. The $SrTiO_3$ 002 and the $YBa_2Cu_3O_7$ 006 reflection were recorded on a back-illuminated deep-depletion CCD camera [26]. The corresponding Bragg angles are $\Theta_{SrTiO_3} = 44.77°$ and $\Theta_{YBa_2Cu_3O_7} = 44.94°$. Two translation stages allowed for precise positioning of the $YBa_2Cu_3O_7$ meander into the x-ray focus. The sample was excited by an 80 fs, 800 nm pump pulse with a fluence of 80 μJ cm^{-2}. Assuming that all the laser energy is transferred into broken pairs, this fluence is 20 times higher than needed to break all Cooper pairs [22]. Even if only 1% of the laser energy is used for destruction of superconductivity, [23], we still break approximately 20% of the pairs. The temperature increase due to the optical pump pulse is estimated to be 7 K at maximum. The coupling between the excited electronic subsystem and the lattice becomes important only after a few ps, and thus a temperature increase in the sample for the investigated delays can be excluded. Further, cumulative effects at the 10 Hz repetition rate does not play a role. In [24], it was estimated that heat diffusion through the $YBa_2Cu_3O_7$ thin film takes about 9 ns and heat

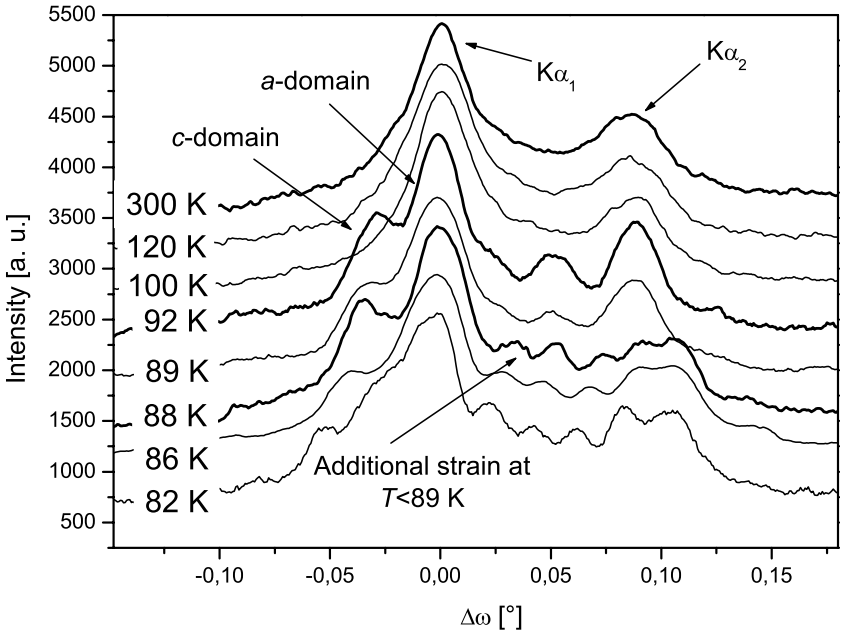

Figure 2. Rocking curves of a $SrTiO_3$ single crystal covered with a thin $YBa_2Cu_3O_7$ film at different temperatures. Significant changes in the strain-related peak structure appear at 92 K (due to the cubic-to-tetragonal phase transition in $SrTiO_3$) and below 89 K. The latter coincides with the superconducting phase transition of the $YBa_2Cu_3O_7$ film and a subsequent increase in the corresponding order parameter.

escape across the interface to the substrate takes another 15 ns. After a few ms the heat has fully dissipated.

We can exclude any optical excitation of the substrate since the $YBa_2Cu_3O_7$ film thickness is about twice the optical absorption length at 800 nm, and the absorption length of $SrTiO_3$ is much larger than 1 m [25].

3. Temperature-dependent measurements

Prior to the time-dependent studies, we investigated the temperature dependence of the sample structure. These diffraction studies were performed with a conventional x-ray tube containing a titanium anode. The setup was similar to the one described above. However, while the size of the x-ray source at the plasma source is about 100 μm [27], the size of the source at the x-ray tube is 400 μm. Further, a Si(311) toroidally bent crystal was used as an x-ray optic. As a consequence, and in contrast to the time-dependent measurements, for the temperature-dependent studies the Kα doublet could not be separated. Both Kα_1 and Kα_2 are reflected by the bent crystal. An Agfa Strukturix x-ray film was used as a detector for the static measurements. The experimental setup does not allow the determination of lattice constants, and relative changes of the lattice constants, and only the shape of the curve can be discussed. The results are shown in figure 2. The two peaks at 300 K are the Kα_1 and Kα_2 $SrTiO_3$ 002 reflections. The position of the Kα_1 peak was set to $\Delta\omega = 0$. The $YBa_2Cu_3O_7$ 006 reflection cannot be resolved due to its much lower reflection power. At 92 K, the two peaks split into four peaks, reflecting the

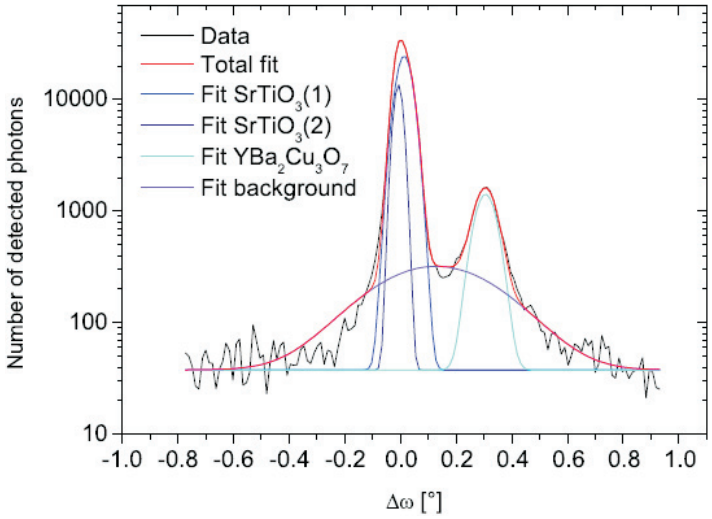

Figure 3. Measured rocking curve of the unpumped sample (accumulated over 2000 pulses) and the corresponding fit functions.

cubic-to-tetragonal phase transition of the $SrTiO_3$ substrate [28]. The observation that at 100 K the tetragonal splitting has not yet occurred is consistent with [29], in which the structural phase transition of $SrTiO_3$ in a near-surface region is investigated in more detail. This work found that, even though the rotation of the oxygen octahedron starts at 105 K, formation of twin domains starts only at lower temperatures, which also depends on external parameters, such as the epitaxial strain. After passing the superconducting transition temperature ($T_c = 89$ K), a number of additional peaks appear, becoming better defined at lower temperatures. The occurrence of these peaks is clear proof of major structural modifications and can only be explained by the build-up of a strong strain field in the substrate. The proximity of the onset of the strain field and the onset of superconductivity in the top layer suggests a relationship between both effects. The shape of the rocking curve further changes as the temperature decreases. As the superconducting order parameter and the energy gap are still increasing at these temperatures, this further supports the suggestion of a common origin for superconductivity and the observed large strain field below 89 K.

4. Time-dependent measurements

Time-dependent studies were performed on a second sample. Thin film thickness, crystalline quality and superconducting transition temperature were similar for both samples. A typical rocking curve at 70 K accumulated over 2000 pulses is shown in figure 3. Two well-separated contributions to the reflection curve are apparent: the main peak arises from the $K\alpha_1$ reflection of the substrate, while the smaller one originates from the thin film. No further peaks are apparent. We attribute their absence to the slightly different sample properties, e.g. different epitaxial strain. However, as will be shown below, this does not lead to a complete disappearance of the strain field related to the onset of superconductivity.

The substrate reflection is slightly asymmetric with a larger weight on the large angle side (compare figure 4). The entire $SrTiO_3$ signal is built up by 190 000 photons, while the $YBa_2Cu_3O_7$ reflection is formed by only about 11 000 photons (each accumulated over 2000

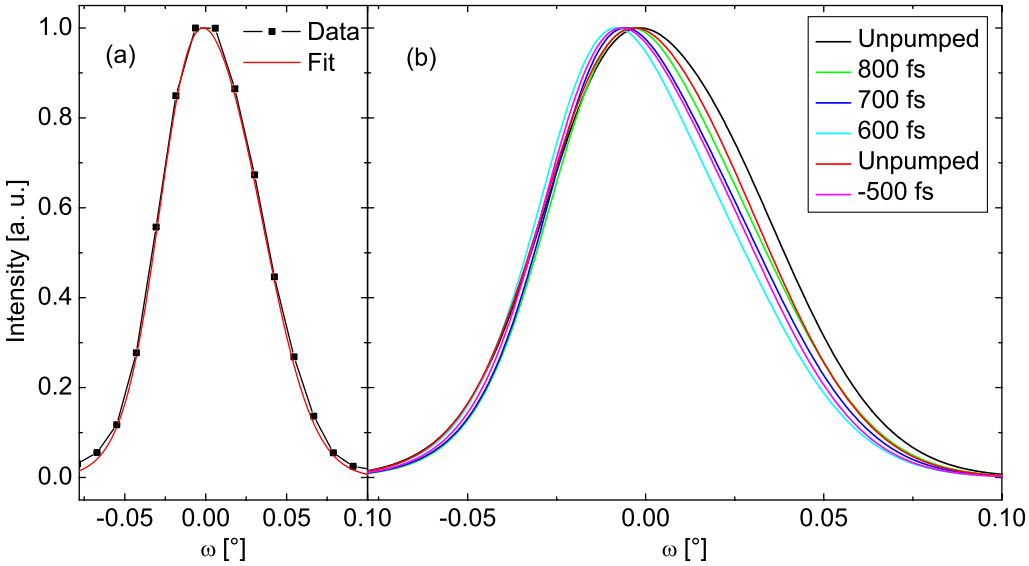

Figure 4. $SrTiO_3$ 002 rocking curves for various delays. For the sake of clarity, fit functions instead of raw data are shown. Data were taken in the same order as listed in the legend. Panel (a) compares an unpumped rocking curve with its fit function and demonstrates very good agreement between both.

pulses). The count rate decreases with increasing operation time of the debris protection in front of the focusing mirror. Therefore, no conclusions from the temporal evolution of the integrated reflectivities can be drawn and all reflection curves are normalized such that the $SrTiO_3$ peak value is set to 1. As the laser intensity also determines the x-ray source size [27], one has to assume that this also changes and leads to a variation in the x-ray focal size. Although the experimental setup allows for very sensitive measurements of changes in the lattice constant, it does not provide an accurate measure for the absolute value of the lattice constant. For further analysis, the measured reflection curve is fitted with four Gaussians (two for the $SrTiO_3$ 002 reflection, one for the $YBa_2Cu_3O_7$ 006 reflection and one for the background).

The time-dependent rocking curves are shown in figure 4. Fit functions rather than raw data are shown as they provide a clearer view. In figure 4(a), the fit function for an unpumped exposure is shown in comparison with the raw data, and very good agreement is obtained. Very similar agreement is found for any other measured reflection curve. The two unpumped reflection curves differ slightly from each other. Apparently, there is a small drift during the measurement. However, the differences between pumped and unpumped exposures are significantly larger than the drift. Upon excitation of the sample, the reflection curve becomes narrower. The main changes to the rocking curve occur on the large angle side, and this leads to an asymmetric narrowing. Further, the reflection curves are slightly shifted towards smaller angles. Figure 5 shows the time dependences of the reflection curve width and peak position (derived from the fit parameters). The data point at $\Delta\tau = -\infty$ is given by the mean of the four unpumped values. The error bar of that data point corresponds to the standard deviation of these four values. Error bars on the other data points are given by the errors of the fit values. Upon breaking Cooper pairs, we observe a distinct decrease in the width of the rocking curve by about 10% and a shift towards smaller angles by about 7×10^{-3} deg. The temporal overlap is known

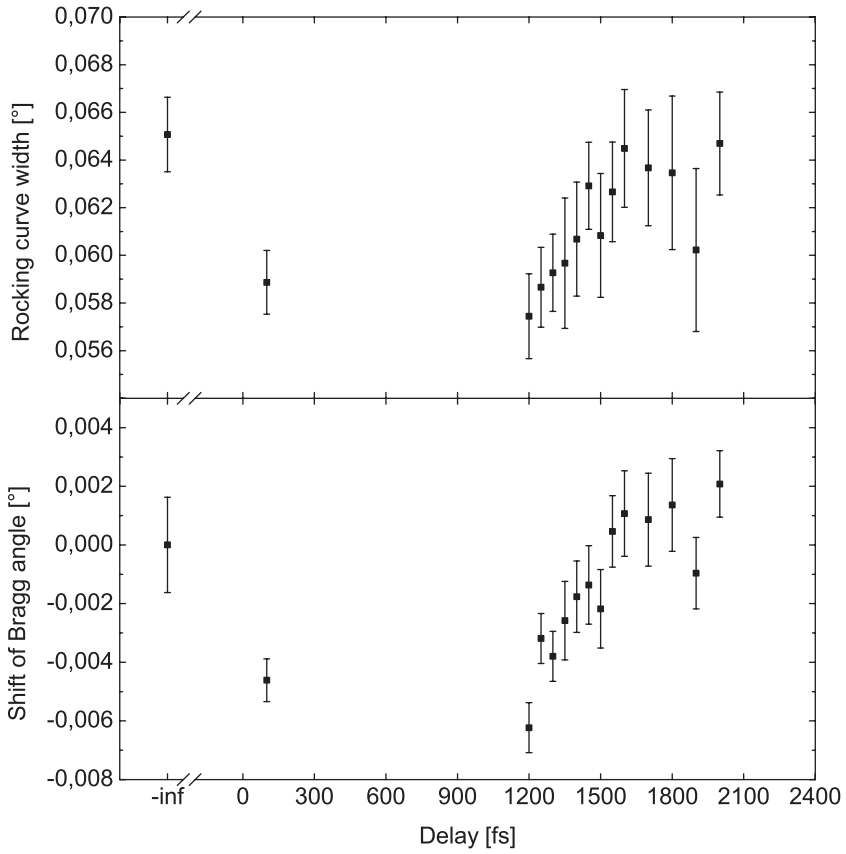

Figure 5. Temporal dependences of the $SrTiO_3$ 002 rocking curve width (upper panel) and peak position (lower panel).

only within a few 100 fs. Therefore, we cannot comment on the characteristic timescale of the initial decrease in the rocking curve width and its shift. However, after 2 ps the initial values are re-established. The time dependences of the width of the rocking curve and the peak shift show similar trends.

5. Data modelling

The asymmetry of the line shape and the reduction in the line width following optical excitation of the sample can be understood if the probed sample volume is initially strained and relaxes after optical excitation.

The rocking curves were modelled in order to gain more information about changes in the strain distribution. In fitting the data, a χ^2 minimization routine was used. The intrinsic rocking curve is calculated for a test strain profile, which is then convoluted with an apparatus function to account for the limited experimental resolution. A Gaussian was used for the apparatus function. The angular position, θ, and the width of the Gaussian, σ, were fitting parameters, accounting for possible shift and size reduction of the x-ray focus on the sample during the experiment. Allowing the apparatus function to vary provides the most suitable way to decouple sample response and apparatus effects. As the experimental rocking curves were normalized,

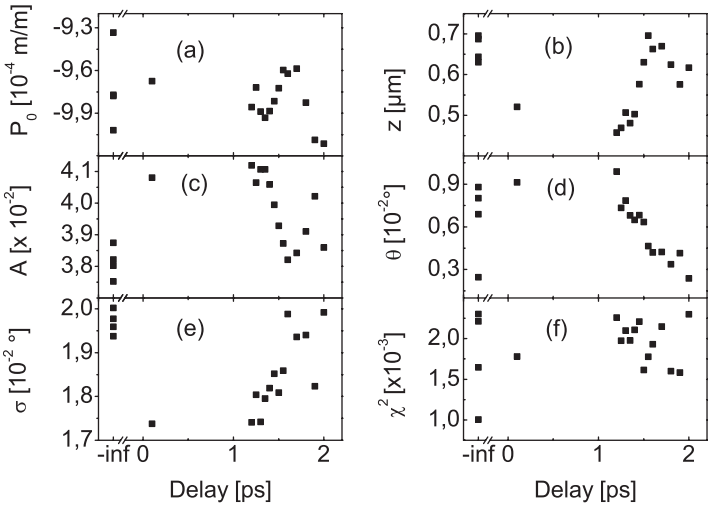

Figure 6. Delay dependence of the fit parameters. (a) The interfacial maximum strain P_0, (b) thickness of the strained $SrTiO_3$ layer z, (c) amplitude A (see text for further explanation), (d) shift of the x-ray focus θ, (e) width of the apparatus function σ and (f) χ^2 of the fit function.

the convolution is multiplied by a factor A, another fitting parameter. The inverse of this factor contains, thus, information about the modelled integrated reflectivity of the sample. The intrinsic rocking curves are calculated in the framework of the dynamical theory of x-ray diffraction as described by Wark *et al* [30].

A linear strain profile is used to model the measured rocking curves. Free parameters are the maximum strain, P_0, at the interface between the thin film and the substrate, and the thickness, z, of the strained layer. In figure 6, the fit parameters are plotted as a function of the delay. The maximum strain (figure 6(a)) randomly varies with delay. The standard deviation of the individual values is 2×10^{-5}, while the average maximum strain is -9.8×10^{-4}. The modelled variation of the strain is at the limit of our high experimental accuracy. The thickness of the strained layer displays a very similar temporal dependence to the measured width and position of the rocking curve. For the unpumped case, the depth of the strained layer is about 650 nm and it is reduced by optical excitation to about 450 nm. Figure 6(c) displays the delay dependence of the convolution's amplitude. Its inverse is a measure of the integrated reflectivity of the sample. This parameter shows the same delay dependence as the strain profile. Figures 6(d) and (e) show the delay dependence of the fitting parameters of the apparatus function. In figure 6(d), the position of the Gaussian is shown. That the trend in θ is nearly linear in the number of data points recorded is apparent. The shift during the entire measurement equals 8×10^{-3} deg. The fitting results also suggest a reduction in the x-ray focal size during the measurement (figure 6(e)). However, as the delay dependence is very similar to that of the strain profile, this might be an artefact of the fitting routine and actually displays, at least partially, changes in the sample rather than of the apparatus function. Finally, in figure 6(f), we show χ^2 of the fit functions. This shows a random variation with delay, indicating that the adopted model sufficiently describes the experiment.

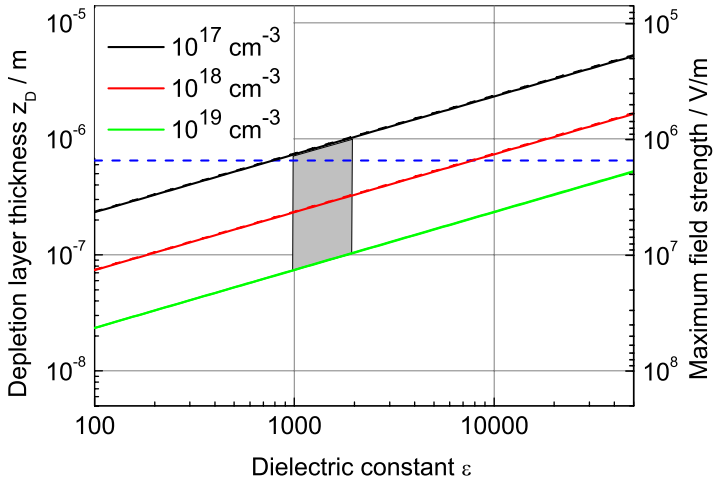

Figure 7. Calculated depletion layer thickness and interface field strength for different carrier densities and dielectric constants. The contact potential is taken as $U_K = 0.5$ V. The grey shaded area corresponds to the expected parameter space. The dashed blue line corresponds to $z_D = 700$ nm, the measured strained layer thickness for the unexcited sample.

6. Discussion

We have shown that a strain field in a $SrTiO_3$ substrate can be made to disappear by heating the sample above the superconducting transition temperature of the $YBa_2Cu_3O_7$ top layer or by ultrafast optical excitation leading to a massive breaking of Cooper pairs. This suggests a close relationship between the existence of this strain field and superconductivity. The thickness of the strained layer in $SrTiO_3$ is of the order of several 100 nm, which is similar to the expected depletion layer, thickness of the Schottky contact. In this depletion layer, a non-vanishing electric field is present. If this layer is strained, piezoelectricity and thus ferroelectricity would be an obvious origin of this strain field. In this case, the strain would be proportional to the electric field strength. For a Schottky contact, the depletion layer thickness is given by $z_D = \sqrt{(2\epsilon\epsilon_0/eN)U_K}$, where ϵ is the dielectric constant, ϵ_0 is the permittivity of free space, N is the carrier density and U_K is the contact potential. The electric field strength at the interface is $E_0 = (e/\epsilon\epsilon_0)Nz_D$. The contact potential is given by the difference in the work functions of the two materials. For $YBa_2Cu_3O_7$, we take a value of 6.1 eV [31]. The band gap of $SrTiO_3$ is 3.2 eV and the electron affinity is 4.1 eV. The Fermi level is close to the center of the gap, which results in a contact potential of about 0.5 V [32]. Typical values for the dielectric constant of $SrTiO_3$ single crystals at 70 K are of the order of 2000 [33]. For thin films, values between 150 and 700 are reported [34, 35]. Thus, we assume that the dielectric constant of the near-surface region of our samples is approximately 1000–2000. Typical carrier densities for non-metallic $SrTiO_3$ thin films and single crystals are in the range of 10^{17}–10^{19} cm^{-3} [36]. In figure 7, we show the expected parameter space. The measured strained layer thickness is well within the range of the expected depletion layer thicknesses and would correspond to carrier densities of about 10^{17} cm^{-3}. Optically breaking Cooper pairs leads to a reduction in the strained layer thickness, but does not alter the strain at the interface between the two materials. If the strained layer thickness is determined by the depletion layer thickness only, this structural response can

only be explained if NU_K/ϵ remains constant. However, at present, we cannot suggest any mechanism that would allow a sub-ps modification of the strained layer thickness under this constraint. Further investigations are needed in order to clarify the origin of the observed strain field.

Acknowledgment

This work was supported by the Deutsche Forschungsgemeinschaft (DFG) within Schwerpunktprogramm 1134.

References

[1] Rose-Petruck C, Jimenez R, Guo T, Cavalleri A, Siders C W, Raksi F, Squier J A, Walker B C, Wilson K R and Barty C P J 1999 Picosecondmilliangstrm lattice dynamics measured by ultrafast X-ray diffraction *Nature* **398** 310

[2] Sokolowski-Tinten K *et al* 2003 Femtosecond X-ray measurement of coherent lattice vibrations near the Lindemann stability limit *Nature* **422** 287

[3] Morak A, Kämpfer T, Uschmann I, Lübcke A, Förster E and Sauerbrey R 2006 Acoustic phonons in InSb probed by time-resolved X-ray diffraction *Phys. Status Solidi.* b **243** 2728

[4] Uschmann I, Kämpfer T, Zamponi F, Lübcke A, Zastrau U, Loetzsch R, Höfer S, Morak A and Förster E 2009 Investigation of fast processes in condensed matter by time-resolved x-ray diffraction *Appl. Phys.* A **96** 91

[5] Siders C W, Cavalleri A, Sokolowski-Tinten K, Toth Cs, Guo T, Kammler M, Horn von Hoegen M, Wilson K R, von der Linde D and Barty C P J 1999 Detection of nonthermal melting by ultrafast X-ray diffraction *Science* **286** 1340

[6] Cavalleri A, Toth Cs, Siders C W, Squier J A, Raksi F, Forget P and Kieffer J. C 2001 Femtosecond structural dynamics in VO_2 during an ultrafast solid–solid phase transition *Phys. Rev. Lett.* **87** 237401

[7] Rousse A *et al* 2001 Non-thermal melting in semiconductors measured at femtosecond resolution *Nature* **410** 65

[8] Sokolowski-Tinten K, Blome C, Dietrich C, Tarasevitch A, Horn von Hoegen M, von der Linde D, Cavalleri A, Squier J and Kammler M 2001 *Phys. Rev. Lett.* **87** 225701

[9] Bargheer M, Zhavoronkov N, Gritsai Y, Woo J C, Kim D S, Woerner M and Elsaesser T 2004 Coherent atomic motions in a nanostructure studied by femtosecond X-ray diffraction *Science* **306** 1771

[10] Korff Schmising C v, Bargheer M, Kiel M, Zhavoronkov N, Woerner M, Elsaesser T, Vrejoiu I, Hesse D and Alexe M 2007 Coupled ultrafast lattice and polarization dynamics in ferroelectric nanolayers *Phys. Rev. Lett.* **98** 257601

[11] Braun M *et al* 2007 Ultrafast changes of molecular crystal structure induced by dipole solvation *Phys. Rev. Lett.* **98** 248301

[12] Korff Schmising C v *et al* 2008 Ultrafast magnetostriction and phonon-mediated stress in a photoexcited ferromagnet *Phys. Rev.* B **78** 060404

[13] Zamponi F, Ansari Z, Woerner M and Elsaesser T 2010 Femtosecond powder diffraction with a laser-driven hard X-ray source *Opt. Express* **18** 947

[14] Hemberger J, Lunkenheimer P, Viana R, Böhmer R and Loidl A 1995 Electric-field-dependent dielectric constant and nonlinear susceptibility in $SrTiO_3$ *Phys. Rev.* B **52** 13159

[15] Uwe H and Sakudo T 1976 Stress-induced ferroelectricity and soft phonon modes in $SrTiO_3$ *Phys. Rev.* B **13** 271

[16] Fuchs D, Schneider C W, Schneider R and Rietschel H 1999 High dielectric constant and tunability of epitaxial $SrTiO_3$ thin film capacitors *J. Appl. Phys.* **85** 7362

[17] Haeni J H *et al* 2004 Room-temperature ferroelectricity in strained $SrTiO_3$ *Nature* **430** 758
[18] Han S G, Vardeny Z V, Wong K. S, Symko O. G and Koren G 1990 Femtosecond optical detection of quasiparticle dynamics in high-T_c $YBa_2Cu_3O_{7-\delta}$ superconducting thin films *Phys. Rev. Lett.* **65** 2708
[19] Albrecht W, Kruse Th and Kurz H 1992 Time-resolved observation of coherent phonons in superconducting $YBa_2Cu_3O_{7-\delta}$ thin films *Phys. Rev. Lett.* **69** 1451
[20] Kaindl R. A, Woerner M, Elsaesser T, Smith D. C, Ryan J. F, Farnan G. A, McCurry M. P and Walmsley D G 2000 Ultrafast mid-infrared response of $YBa_2Cu_3O_{7-\delta}$ *Science* **287** 470
[21] Li E, Sharma R P, Ogale S B, Zhao Y G, Venkatesan T, Li J J, Cao L W and Lee C H 2002 Sharp resonant multiplet in femtosecond optical pair-breaking spectroscopy of optimally doped, underdoped, and Zn-doped $YBa_2Cu_3O_{7-\delta}$: Transient insulating regions in the superconducting state *Phys. Rev.* B **65** 184519
[22] Mazin I I, Liechtenstein A I, Jepsen O, Andersen O K and Rodriguez C O 1994 Displacive excitation of coherent phonons in $YBa_2Cu_3O_{7-\delta}$ *Phys. Rev.* B **49** 9210
[23] Zhao Y G *et al* 1999 Unusual photon energy dependence of the Cooper pair breaking rate in $YBa_2Cu_3O_{7-\delta}$ epitaxial thin films *J. Supercond.* **12** 675
[24] Wald H 2003 Optoelektronische Bauelemente auf Basis von Dünnschichtsystemen mit Hochtemperatur-supraleitern *Dissertation* Friedrich-Schiller-Universität Jena
[25] Cardona M 1965 Optical properties and band structure of $SrTiO_3$ and $BaTiO_3$ *Phys. Rev.* A **140** 651
[26] Zamponi F, Kämpfer T, Morak A, Uschmann I and Förster E 2005 Characterization of a deep depletion, back-illuminated charge-coupled device in the x-ray range *Rev. Sci. Instrum.* **76** 116101
[27] Reich C, Uschmann I, Ewald F, Düsterer S, Lübcke A, Schwoerer H, Sauerbrey R, Förster E and Gibbon P 2003 Spatial characteristics of Kα X-ray emission from relativistic femtosecond laser plasmas *Phys. Rev.* E **68** 056408
[28] Shirane G and Yamada Y 1969 Lattice-dynamical study of the 110 K phase transition in $SrTiO_3$ *Phys. Rev.* **177** 858
[29] Loetzsch R, Lübcke A, Uschmann I, Förster E, Große V, Thürk M, Köttig T, Schmidl F and Seidel P 2010 The cubic to tetragonal phase transition in $SrTiO_3$ single crystals near its surface under internal and external strains *Appl. Phys. Lett.* **96** 071901
[30] Wark J, Whitlock R R, Hauer A A, Swain J E and Solone P J 1989 Subnanosecond x-ray diffraction from laser-shocked crystals *Phys. Rev.* B **40** 5705
[31] Hirano T, Ueda M, Matsui K, Fujii T, Sakuta K and Kobayashi T 1992 Dielectric properties of $SrTiO_3$ epitaxial film and their application to measurement of work function of $YBa_2Cu_3O_y$ epitaxial film *Japan J. Appl. Phys.* **31** L1345
[32] Henrich V E, Dresselhaus G and Zeiger H J 1978 Surface defects and the electronic structure of $SrTiO_3$ surfaces *Phys. Rev.* B **17** 4908
[33] Mueller K A and Burkard H 1979 $SrTiO_3$: an intrinsic quantum paraelectric below 4 K *Phys. Rev.* B **19** 3593
[34] Gao Y-H, Cao H-X and Jiang Q 2005 Effect of misfit strain and external electric field on dielectric behaviour of epitaxial $SrTiO_3$ thin films *J. Appl. Phys.* **97** 064109
[35] Sirenko A A, Bernhard C, Golnik A, Clark A. M, Hao J, Si W and Xi X X 2000 Soft-mode hardening in $SrTiO_3$ thin films *Nature* **404** 373
[36] Ohtomo A and Hwang H Y 2007 Growth mode control of the free carrier density in $SrTiO_{3-\delta}$ films *J. Appl. Phys.* **102** 083704